ENHANCED DISSOLUTION OF TRICHLOROETHYLENE-CONTAMINATED SOIL WITH SODIUM DODECYL SULFATE-CONTAINING SOLUTION

Yi-Hung Chen,[1,]* Ching-Yuan Chang,[2] Je-Lueng Shie,[3] Chyow-San Chiou,[3] Fi-John Chang,[4]

Rong-Hsien Lin[5] and Chun-Yu Chiu[6]

[1] Department of Chemical Engineering and Biotechnology
National Taipei University of Technology
Taipei 106, Taiwan
[2]Graduate Institute of Environmental Engineering
National Taiwan University
Taipei 106, Taiwan
[3]Department of Environmental Engineering
National Ilan University
Yilan 260, Taiwan
[4]Department of Bioenvironmental Systems Engineering
National Taiwan University
Taipei 106, Taiwan
[5]Department of Chemical and Material Engineering
National Kaohsiung University of Applied Sciences
Kaohsiung 807, Taiwan
[6]Department of Cosmetic Science and Application
Lan-Yang Institute of Technology
I-Lan 261, Taiwan

Key Words: Trichloroethylene, sodium dodecyl sulfate, groundwater, remediation, dynamic model

ABSTRACT

The dynamic behavior of sodium dodecyl sulfate (SDS)-enhanced solubilization for the removal of trichloroethylene (TCE) from the contaminated soil is studied. Several remediation processes of the TCE-contaminated soil in the columns were carried out by flushing with the SDS-containing solution of various concentrations under different experimental conditions. The concentration variations of SDS and TCE in the effluent solution were analyzed during the course of the experiments. As a remediation process started, the TCE cumulated on the soil was dissolved gradually as the organic solute into the solution and was removed by the solubilization mechanism. There exist dynamic variations of SDS and TCE concentrations in the solution and residual TCE volumetric fraction on the soil during the remediation process. The case with higher SDS concentration and high flow rate of solution can accomplish the complete remediation faster. In addition, a dynamic axial dispersion model was proposed to predict the transient concentration and volumetric fraction profiles of TCE along the column. The relationship between the TCE-aqueous mass transfer rate parameter and SDS concentration as well as solution flow rate is presented according to the experimental results. Further, the effects of the dimensionless system parameters, such as the Peclet number (Pe_L), Stanton number (St_{OA}), and molar solubilization ratio on the performance of surfactant-enhanced solubilization for the remediation process are also examined. As a result, the study provides the useful information about the dynamic behavior of the SDS-enhanced solubilization in the TCE-contaminated soil.

INTRODUCTION

The emission of non-aqueous phase liquids (NAPLs) from the contaminated sites, which migrates vertically through the unsaturated zone to reach the aquifer layer as a discrete liquid phase, endangers the quality of groundwater due to their high toxic and carcinogenic potential properties. The common NAPLs include the pesticides, alkanes, chlorinated solvents, polycyclic biphenyls and polycyclic aromatic hydro-

*Corresponding author
Email: yhchen1@ntut.edu.tw

carbons [1]. The NAPLs being as the organic solutes with the small water solubilities and slow dissolution rates into the groundwater represent a long-term source of contamination [2]. However, the convectional remediation technique such as the pump-and-treat method is not efficient for the clean up of the contaminated sites within the reasonable time period [3,4].

The pump-and-treat treatment combined with the surfactant-enhanced solubilization has been considered as the practicable remediation process [5-7]. The solubility of NAPLs would apparently increase with the addition of surfactant with the surfactant concentration above its critical micelle concentration (CMC) [8,9]. At the surfactant concentration above the CMC, the surfactant molecules start to aggregate and form the micelles. The surfactant-containing solution is capable of enhancing the solubility of immiscible NAPLs by the partition of organic solutes into the micelles. Thereby the time required for the elimination of the NAPLs in the contaminated soil can be significantly reduced [10].

Trichloroethylene (TCE) considered as one of the most common NAPLs is usually used as a solvent to remove grease from metal parts as well as an ingredient in adhesives, paint removers, and typewriter correction fluids. TCE with the small water solubility can remain in groundwater for a long time, while drinking the TCE-containing solution may cause nausea, liver damage, unconsciousness, and impaired heart function [11,12]. On the other hand, sodium dodecyl sulfate (SDS) is an ionic surfactant that has been employed in the remediation of groundwater. The SDS molecule with a tail of 12 carbon atoms attached to a sulfate group has the amphiphilic properties [13]. Furthermore, SDS is considered with good properties with respect to the low toxicity to human exposure.

The aim of this study is to investigate the dynamic processes of SDS-enhanced solubilization for the remediation of the TCE-contaminated soil. The remediation of the TCE-contaminated soil packed in the columns is preceded under different operating conditions. It should be addressed that the introduction of the surfactant in the remediation process may affect both the solubility of NAPL and the NAPL-aqueous mass transfer rate simultaneously. Therefore, one model is proposed to incorporate the transport equations for the organic solute and surfactant in the aqueous phase accompanying with the mass balance of the residual NAPLs in the contaminated soil. The validity of the model is demonstrated by the good agreement of the predicted results with the experimental data. The determination coefficient (R^2) which represents the consistency between the predicted values (C_p) and the experimental ones (C_e) is employed to determine the parameter values. The values of the hydrodynamic and mass transfer rate parameters are estimated accordingly. Furthermore, the correlation of

the mass transfer rate parameter associated with the SDS concentration and water flow rate has been obtained. For the engineering design, the effects of the dimensionless system parameters on the efficiency of the remediation process are also examined. Compared to the previous studies about the groundwater remediation, this study presents more comprehensive description about the effects of the dimensionless system parameters. Consequently, the results in this study provide the useful information about the dynamic behavior of SDS-enhanced solubilization for the TCE removal in the contaminated soil.

THEORETICAL ANALYSIS

1. Equilibrium of Organic Solute in Micellar Solution

The solubilization capacity for an organic solute in a surfactant-containing solution can be quantified by the molar solubilization ratio (MSR), which is a ratio of the mol of an organic solute B solubilized in the micelles to the mol of surfactant S in micellar form. The equilibrium concentration of the organic solute in the bulk solution (C_{BA}^{eq}) is enhanced when the surfactant concentration (C_{SA}) is higher than its CMC (C_{cmc}). Thus the dimensionless C_{BA}^{eq} value ($\theta_{BA}^{eq} = C_{BA}^{eq} / C_{BW}^{sat}$) can be calculated from the MSR and dimensionless C_{SA} value ($\theta_{SA} = C_{SA}/C_{cmc}$) using Eq. 1 [14], where C_{BW}^{sat} is the solubility of the organic solute in the bulk solution.

$$\theta_{BA}^{eq} = 1 + MSR\left(\frac{C_{cmc}}{C_{BW}^{sat}}\right)(\theta_{SA} - 1) \qquad (1)$$

For the saturated aquifer, the volumetric fraction of the aqueous phase (ϕ_A) can be expressed by Eq. 2. ϕ_P and ϕ_O are the volumetric fractions of porosity and NAPL in the saturated aquifer, respectively.

$$\phi_A = \phi_P - \phi_O \qquad (2)$$

1.2. Surfactant-enhanced Solubilization Model

A dynamic axial dispersion model is developed to describe the dynamic variations of dimensionless organic solute ($\theta_{BA} = C_{BA}/C_{BW}^{sat}$) and surfactant ($\theta_{SA}$) concentrations in the aqueous phase, and ϕ_O where C_{BA} is the concentration of organic solute in the bulk solution. The hydrodynamic characteristic of the system is considered for the concentration profiles. Furthermore, the sorption of the surfactant on the soil is negligible [15-17]. Assuming the homogeneous soil properties and a uniform distribution of the ϕ_O at the initial time, the governing equations for the surfactant-enhanced solubilization of NAPL are derived from the mass balance concept including the solute dispersion, fluid convection, and interface mass transfer as follows.

For θ_{BA}:

$$\frac{\partial \theta_{BA}}{\partial \tau} = \frac{1}{\phi_A} \left[\frac{\partial}{\partial z^*} \left(\frac{\phi_A}{Pe_L} \frac{\partial \theta_{BA}}{\partial z^*} \right) - \frac{\partial(\phi_A U_A \theta_{BA})}{\partial z^*} + \right.$$

$$\left. St_{OA} \left(\theta_{BA}^{eq} - \theta_{BA} \right) - \theta_{BA} \frac{\partial \phi_A}{\partial \tau} \right] \quad (3)$$

For θ_{SA}:

$$\frac{\partial \theta_{SA}}{\partial \tau} = \frac{1}{\phi_A} \left[\frac{\partial}{\partial z^*} \left(\frac{\phi_A}{Pe_L} \frac{\partial \theta_{SA}}{\partial z^*} \right) - \frac{\partial(\phi_A U_A \theta_{SA})}{\partial z^*} - \theta_{SA} \frac{\partial \phi_A}{\partial \tau} \right] \quad (4)$$

In Eqs. 3 and 4, the left-hand side terms represent the concentration variations in the aqueous phase, while the right-hand side terms stand for the effects of the dispersion, convection, NAPL-aqueous mass transfer, and the ϕ_A variation, respectively. The dimensionless time (τ) and axial coordinate (z^*) are calculated as t/t_L and z/L, respectively, where t and z are time and axial coordinate of column, respectively. t_L, the hydraulic retention time, is defined as the length of column (L) divided by the superficial velocity of the aqueous phase (q). The value of q is calculated as the volumetric flow rate of the aqueous phase divided by the column cross area. In addition, the dimensionless actual velocity of the aqueous phase ($U_A = v_A/q$) can be obtained as ϕ_A^{-1}. The v_A is the actual velocity of the aqueous phase.

In the above equations, the definitions of the dimensionless variables and parameter groups are listed in the nomenclature. The Peclet number (= Lq/D_H) represents the hydrodynamics. For the small Pe_L value, the hydraulic condition behaves like the complete mixing. On the contrary, the hydraulic condition changes to the plug flow with the increase of the Pe_L value [18]. The hydrodynamic dispersion coefficient (D_H) can be taken as $D_H = \alpha_L v_A$, where the α_L is the longitudinal dispersivity [15,16].

The Stanton number (= $k_f a_e L/q$) stands for the signification of the NAPL-aqueous mass transfer rate of the organic solute. The overall NAPL-aqueous mass transfer coefficient ($k_f a_e$) can be substituted by the product of the NAPL-aqueous mass transfer rate parameter (k_1) and the factor of the aqueous saturation $\left(S_A^3 - S_A^5 \right)$ as $k_f a_e = k_1 \left(S_A^3 - S_A^5 \right)$, where k_f, a_e, and S_A are the NAPL-aqueous mass transfer coefficient of organic solute, the specific NAPL-aqueous interfacial area based on the total volume, and the aqueous saturation defined as $\phi_A /(\phi_A + \phi_O)$, respectively [16]. Note that the variation of the a_e is dynamic and proportional to the $\left(S_A^3 - S_A^5 \right)$. Furthermore, the presence of the surfactant may affect the interfacial tension and mass transfer of the NAPL-aqueous interface. The k_1 value is used to account for the effects of those phenomena in the present model.

For ϕ_O:

$$\frac{\partial \phi_O}{\partial \tau} = -St_{OA} \frac{\left(\theta_{BA}^{eq} - \theta_{BA} \right)}{\theta_{BO}} \quad (5)$$

The initial conditions of Eqs. 3-5 are

$$\tau = 0$$
$$\theta_{BA} = \theta_{BA}^0$$
$$\theta_{SA} = 0 \quad (6)$$
$$\phi_O = \phi_O^0$$

where $\theta_{BA}^0 = C_{BA}^0 / C_{BW}^{sat}$ in which C_{BA}^0 is the initial concentration of organic solute in bulk solution. ϕ_O^0 is the initial volumetric fraction of NAPL.

The boundary conditions of Eqs. 3 and 4:

At the inlet, $z^* = 0$:

$$\theta_{BA} = \frac{\phi_A}{Pe_L} \frac{\partial \theta_{BA}}{\partial z^*}$$
$$\quad (7)$$
$$\theta_{SA} = \theta_{SA}^0 + \frac{\phi_A}{Pe_L} \frac{\partial \theta_{SA}}{\partial z^*}$$

where $\theta_{SA}^0 = C_{SA}^0 / C_{cmc}$ in which C_{SA}^0 is the influent surfactant concentration.

At the outlet, $z^* = 1$:

$$\frac{\partial \theta_{BA}}{\partial z^*} = \frac{\partial \theta_{SA}}{\partial z^*} = 0 \quad (8)$$

Another dimensionless time named pore volumes (PV) is commonly introduced as the characteristic time. PV defined as the flushing volume of the surfactant-containing solution divided by the pore volume of the column is calculated as PV = τ/ϕ_P.

The governing equations with the corresponding initial and boundary conditions are solved by the explicit finite-difference with Turbo C program. The computation is conducted up to the complete elimination of NAPL as θ_{BA} becomes smaller than 10^{-4}. The grids along $z^* = 0$ to 1 and the size of the time step adopted in the program were 101 points and 10^{-4}, respectively. The confidential error range of the numerical mass balance check is less than 10^{-6}. Some modeling parameters including the C_{BW}^{sat} and the MSR value of TCE in the SDS micellar solution are predetermined as 1198 mg L^{-1} and 0.34, respectively, from the previous studies [19,20]. The kinematic viscosity of water (v_a) and diffusion coefficient of TCE (D_L) are taken as 1.3×10^{-6} m^2 s^{-1} and 9.3×10^{-10} m^2 s^{-1}, respectively [21].

EXPERIMENTAL METHODS

1. Chemicals

TCE with chemical formula as C_2HCl_3, which was purchased from Aldrich (Milwaukee, WI, USA) with CAS registry number of 79-01-6, has molecular weight and density of 131.4 g mol^{-1} and 1.465 g cm^{-3}, respectively, according to the manufacturer. SDS was purchased from Riedel-de Haen with the molecular weight and C_{cmc} of 288 g mol^{-1} and 0.00826 M, respectively [22]. All experimental solutions were prepared by the deionized water without other buffers. The conductivity of deionized water used was less

than 1 μS cm^{-1}.

2. Instrumentation

The column of 4.8 cm inside diameter was made of Pyrex glass equipped with water jacket to maintain a constant solution temperature at 25 °C in all experiments. The column packed with the sieved silica sand of the average diameter (d_p) as 6.0 x 10^{-4} m had the immersed height (L) and porosity (ϕ_P) of 0.16 m and 0.31, respectively. Two pumps were set to transport the solution into and out of the column with the controllable flow rates. All fittings, tubings, and bottles were made of stainless steel, Teflon, or glass.

The TCE concentration (C_{BA}) was analyzed using high performance liquid chromatography (HPLC) system with 250 x 4.6 mm model BDS C18 (5 μm) column (Thermo Hypersil-keystone, Bellfonte, PA, USA), and UV/Visible detector (model 1706, Bio-Rad, Hercules, CA, USA) at 212 nm [23]. The effluent solution with flow rate of 1.0 mL min^{-1} had the composition with water: acetonitrile of 12:88. The injection volume of the analytic solution was 20 μL. The C_{SA} in the TCE-free solution was measured by the value of the total organic carbons (TOCs). The TOC value of the sample was analyzed by a TOC analyzer (model 700, O. I. Corporation, Texas, USA).

3. Experimental Procedures

There have been numerous studies mentioned about the value of α_L in the porous mediate system [15-17,24]. Their results indicate that the α_L value is a function of q, column diameter, solution properties, and porosity. In this study, the continuous-injection tracer tests in the TCE-free system were conducted to examine the hydrodynamic characteristic. SDS was directly chosen as the aqueous tracer due to its low volatility and easy quantification by the measurements. The value of α_L was determined according to the residence time distribution of SDS concentration in the effluent solution ($C_{SA,eff}$).

For the remediation tests, the sieved silica sand was packed and saturated with deionized water over night in the columns to minimize the nonwetting region. Then the TCE liquid was introduced into the top of the column using a syringe with the flow rate of 1 mL min^{-1}. When approximate 10% of the pore volume was occupied by TCE liquid, the deionized water was pumped into the top of the column within 6 h. The column was completely saturated by flushing with 20 PV of deionized water. Any TCE existing as the mobile phase was sequentially displaced from the column. The φ_O^0 value of TCE was estimated according to the flushed TCE amount.

The experiments of the SDS-enhanced solubilization were proceeded with different influent SDS concentration (C_{SA}^0) and q. Three θ_{SA}^0 was set as 0, 3,
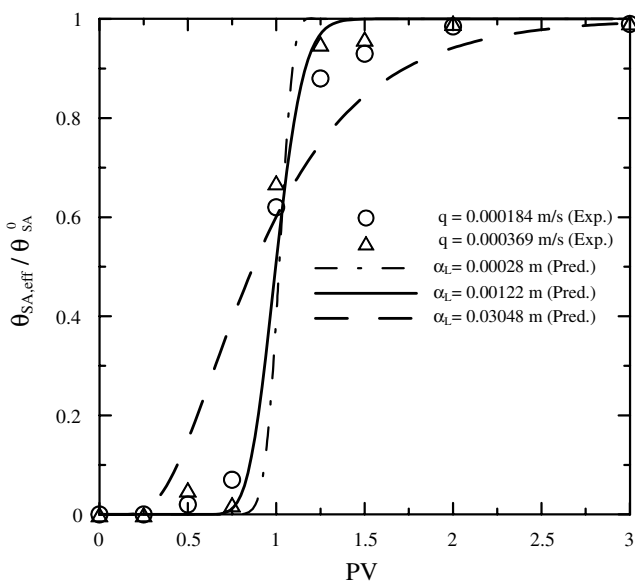

Fig. 1. Variations of $\theta_{SA,eff}$ / θ_{SA}^0 with PV for continuous injection of SDS-containing solution in TCE-free columns. Experimental conditions: θ_{SA}^0 = 3.0, L = 0.16 m, ϕ_O^0 = 0.0, ϕ_P = 0.31. Symbols, lines: experiments, prediction. ○: q = 1.84 x 10^{-4} m s^{-1} (t_L = 868 s); △ : q = 3.69 x 10^{-4} m s^{-1} (t_L = 434 s). ———— : α_L = 0.00122 m determined by experimental data with Pe_L = 40.66 (R^2 = 0.987). —— —— : α_L = 0.03048 m proposed by [23] (Pe_L = 1.63). —— · —— : α_L = 0.00028 m proposed by [14] (Pe_L = 177.1).

10 and 15 at q = 1.84 x 10^{-4} m s^{-1}. Furthermore, two additional q of 9.22 x 10^{-5} and 3.69 x 10^{-4} m s^{-1} were proceeded to test the effect of q at θ_{SA}^0 =3. The value of t_L was estimated between 434 to 1736 s with respect to the adopted q values. Before starting the SDS-enhanced solubilization experiments, the column was held for 12 h to make the initial TCE concentration in the aqueous phase reaching the equilibrium (θ_{BA}^0 =1). Afterwards the SDS-containing solution with the preset flow rate was directed into the top of the column, and the samples were drawn out from the effluent at desired intervals in the course of the experiment for the following analysis.

RESULTS AND DISCUSSION

1. SDS-enhanced Solubilization in TCE-contaminated Soil

The variations of the normalized effluent SDS concentration ($\theta_{SA,eff}$ / θ_{SA}^0) with PV for two cases of different q are depicted in Fig. 1. The $\theta_{SA,eff}$ / θ_{SA}^0 value starts to appear at PV of about 0.5 and reaches to the constant of unity when the PV is greater than 2. It is apparent that the $\theta_{SA,eff}$ / θ_{SA}^0 profile is slightly dependent on q. The α_L value adopted for the simulation is 1.22 x 10^{-3} m by fitting the breakthrough curves
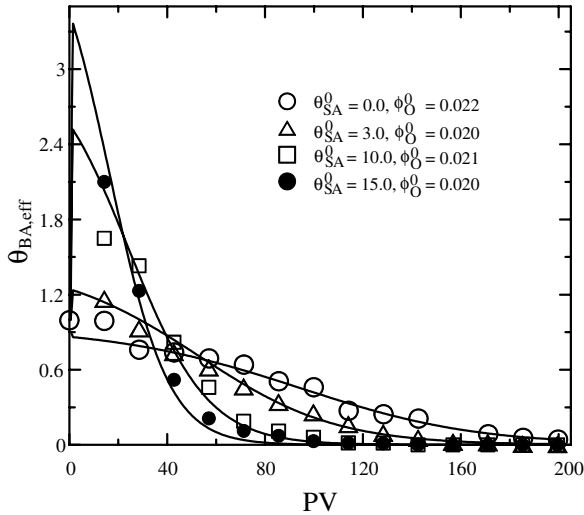
Fig. 2. Concentration variations of $\theta_{BA,eff}$ with PV at various θ_{SA}^0 for SDS-enhanced solubilization in TCE-contaminated columns. Experimental conditions: $\theta_{BA}^0 = 1.0$, $q = 1.84 \times 10^{-4}$ m s^{-1}, $t_L = 868$ s, $L = 0.16$ m, $\phi_P = 0.31$, MSR = 0.34. Symbols, lines: experiments, prediction. ○: $\theta_{SA}^0 = 0.0$, $\phi_O^0 = 0.022$ with prediction line of $Pe_L^0 = 37.77$ and $St_{OA}^0 = 2.001$. △: $\theta_{SA}^0 = 3.0$, $\phi_O^0 = 0.020$ with prediction line of $Pe_L^0 = 38.03$ and $St_{OA}^0 = 1.464$. □: $\theta_{SA}^0 = 10.0$, $\phi_O^0 = 0.021$ with prediction line of $Pe_L^0 = 37.90$ and $St_{OA}^0 = 1.123$. ●: $\theta_{SA}^0 = 15.0$, $\phi_O^0 = 0.020$ with prediction line of $Pe_L^0 = 38.03$ and $St_{OA}^0 = 0.931$. $R^2 = 0.950$, 0.991, 0.980 and 0.986.

Fig. 3. Concentration variations of $\theta_{BA,eff}$ with PV at various q for SDS enhanced-solubilization in TCE-contaminated columns. Experimental conditions: $\theta_{BA}^0 = 1.0$, $\theta_{SA}^0 = 3.0$, $L = 0.16$ m, $\phi_P = 0.31$, MSR = 0.34. Symbols, lines: experiments, prediction. ○: $q = 9.22 \times 10^{-5}$ m s^{-1}, $\phi_O^0 = 0.019$, $t_L = 1736$ s with prediction line of $Pe_L^0 = 38.16$ and $St_{OA}^0 = 1.945$. △: $q = 1.84 \times 10^{-4}$ m s^{-1}, $\phi_O^0 = 0.020$, $t_L = 868$ s with prediction line of $Pe_L^0 = 38.03$ and $St_{OA}^0 = 1.464$. □: $q = 3.69 \times 10^{-4}$ m s^{-1}, $\phi_O^0 = 0.018$, $t_L = 434$ s with prediction line of $Pe_L^0 = 38.30$ and $St_{OA}^0 = 0.977$. $R^2 = 0.977$, 0.991 and 0.996.

of $\theta_{SA,eff}/\theta_{SA}^0$ based on the proposed model. One may note that the magnitude of the α_L value in this work as well as the previous literatures is in the range of 10^{-4} to 10^{-2} m [15-17,24]. Furthermore, two breakthrough curves with the α_L values of 2.8×10^{-4} and 3.05×10^{-2} m proposed by Taylor et al. [17] and Ouyang et al. [24], respectively, are shown in Fig. 1 for comparison. The times for the appearance and breakthrough of the $\theta_{SA,eff}/\theta_{SA}^0$ would be smaller and longer, respectively, with the increase of the α_L value. Obviously, the surfactant concentration in the soil system usually takes PV of 1 to 3 for reaching the steady state that depends on the Pe_L value.

As for the SDS-enhanced solubilization in the TCE-contaminated columns with various θ_{SA}^0, the variations of the dimensionless TCE concentration in the effluent solution ($\theta_{BA,eff} = C_{BA,eff}/C_{BW}^{sat}$) are shown in Fig. 2 where $C_{BA,eff}$ is the concentration of organic solute in the effluent solution. Apparently, the case of higher θ_{SA}^0 significantly enlarges the $\theta_{BA,eff}$ value in the initial period (say PV smaller than 30) and accomplishes the complete remediation within a shorter period. It is because that the higher θ_{SA}^0 leads to the higher θ_{BA}^{eq} resulting in the faster TCE-aqueous mass transfer rate. As a result, the time required for the $\theta_{BA,eff}$ to decrease below the detection limit of
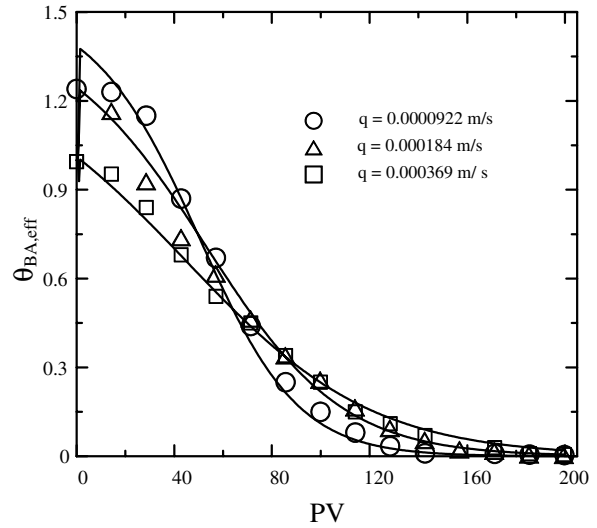
TCE can be reduced 53-64% by employing the SDS-enhanced solubilization compared to the pure water flush. In addition, the dynamic variations of $\theta_{BA,eff}$ with various q at $\theta_{SA}^0 = 3.0$ are shown in Fig. 3. The $\theta_{BA,eff}$ would have the smaller initial value and decrease slower with PV at the higher q. However, it has to be clarified that the actual time for the remediation process with the higher q is remarkably shorter due to its smaller t_L.

For the further investigation, the variations of the $\theta_{BA,eff}$ in the experiments with various θ_{SA}^0 and q are simulated by the proposed model. The $\theta_{BA,eff}$ value is predicted based on the proper value of k_1 for the best fitting. As indicated in Figs. 2 and 3, the prediction of the $\theta_{BA,eff}$ shows the good agreement with the experimental data from the beginning to the end. The k_1 values for the SDS-enhanced solubilization processes in the TCE-contaminated columns are listed in Table 1. It is distinct that the value of k_1 depends on both θ_{SA}^0 and q. The k_1 value would increase with the higher q due to the compression of the TCE-aqueous interfacial film. On the contrary, the k_1 value remarkably decreases with the increase of θ_{SA}^0. This phenomenon is caused by the increasing resistance of the TCE–aqueous mass transfer because that the more surfactant monomers are adsorbed onto the TCE-aqueous in-

Table 1. NAPL-aqueous mass transfer rate parameter of SDS-enhanced solubilization in TCE-contaminated column under different conditions[a]

Run no.	$q \times 10^4$ (m s^{-1})	θ_{SA}^0 (-)	ϕ_O^0 (-)	k_1 (s^{-1})	Re[b]	Sh[c]
1	0.922	3.0	0.019	0.0114	0.0425	4.41
2	1.84	0.0	0.022	0.0210	0.0851	8.13
3	1.84	3.0	0.020	0.0165	0.0851	6.39
4	1.84	10.0	0.021	0.0122	0.0851	4.72
5	1.84	15.0	0.020	0.0116	0.0851	4.32
6	3.69	3.0	0.018	0.0239	0.170	9.25

[a]: $\phi_P = 0.31$; $L = 0.16$ m; $d_p = 6.0 \times 10^{-4}$ m.
[b]: $Re = d_p q / \nu_a$.
[c]: $Sh = k_1 d_p^2 / D_L$.

terfacial surface at higher θ_{SA}^0 [25-27].

Furthermore, the expression of the NAPL-aqueous mass transfer coefficient (k_f) can be described by Eq. 9 [28]. The k_L^{-1} and k_S^{-1} are denoted as the mass transfer resistance of the liquid and surfactant films, respectively.

$$\frac{1}{k_f} = \frac{1}{k_L} + \frac{1}{k_S} \qquad (9)$$

Moreover, the k_S^{-1} value is assumed to have the relationship with θ_{SA}^0 as $1/k_s \sim (\theta_{SA}^0)^m$. Then the correlation for the modified Sherwood number (Sh = $k_1 d_p^2 / D_L$ or $k_f a_e (S_A^3 - S_A^5)^{-1} d_p^2 / D_L$) can be obtained as Eq. 10 according to the results in Table 1. The effect of q on the Sh is represented by the Reynolds number (Re = $d_p q / \nu_a$) [15,21].

$$Sh = \frac{30.3}{1 + 0.118(\theta_{SA}^0)^{0.760}} Re^{0.534} \qquad (10)$$

Comprising with the power of Re in the previous correlation for the Sherwood number ranging from 0.20 to 1.04 [15-17,25,29], the power of Re in Eq. 10 as 0.53 is considered reasonable. However, the effect of the surfactant concentration on the Sherwood number in the previous studies was usually lacked.

2. Simulation of Dynamic Processes of Surfactant-enhanced Solubilization

To characterize the dynamic processes during the surfactant-enhanced solubilization of the contaminated soil, the values of the modeling parameters in the following simulation are the same as those specified in Fig. 2 at $\theta_{SA}^0 = 3.0$. As shown in Fig. 4, the profiles of θ_{BA} and ϕ_O are the functions of the dimensionless axial coordinate z^* and time τ. The values of θ_{BA} and ϕ_O monotonically increase with z^* along the column. Thus the maximum values of θ_{BA} and ϕ_O would occur in the effluent solution. In addition, the values of the θ_{BA} and ϕ_O decrease slower with τ in the late stage of the process. It can be elucidated by the variation of the $(S_A^3 - S_A^5)$, which has the maximum value of 0.19 at $\phi_O = 0.07$ and decreases with the smaller ϕ_O.
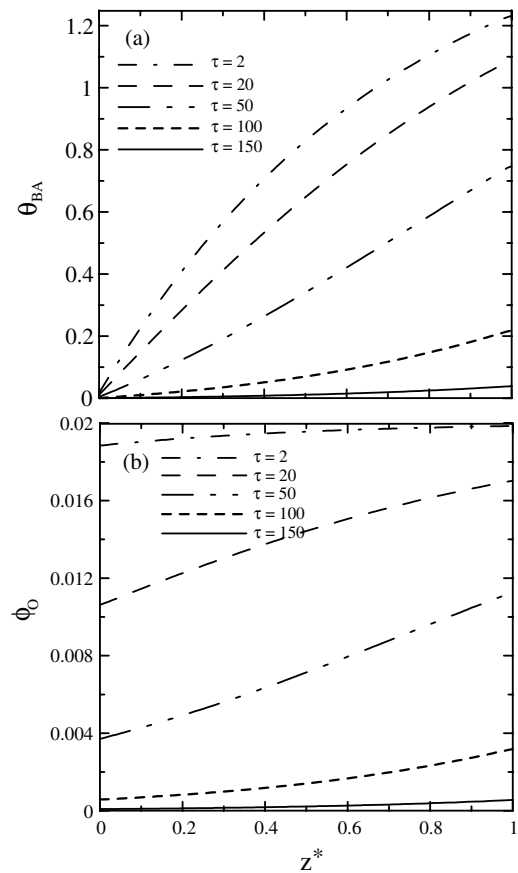

Fig. 4. Profiles of θ_{BA} and ϕ_O with z^* at different τ for SDS-enhanced solubilization in TCE-contaminated column. $\theta_{BA}^0 = 1.0$, $\theta_{SA}^0 = 3.0$, q = 1.84×10^{-4} m s^{-1}, $t_L = 868$ s, L = 0.16 m, $\phi_O^0 = 0.020$, $\phi_P = 0.31$ ($Pe_L^0 = 38.03$, $St_{OA}^0 = 1.464$, MSR = 0.34). Lines: prediction. — · —, — —, — ·· —, – – – – and ———: τ = 2, 20, 50, 100 and 150. (a) θ_{BA} and (b) ϕ_O.

To show the effects of the dimensionless system parameters on the dynamic processes of the surfactant-enhanced solubilization, Figs. 5-7 depict the time variations of the $\theta_{BA,eff}$ and average value of ϕ_O along the column ($\phi_{O,avg}$) at various levels of Pe_L, St_{OA}, and MSR, respectively, while the other parameters are the
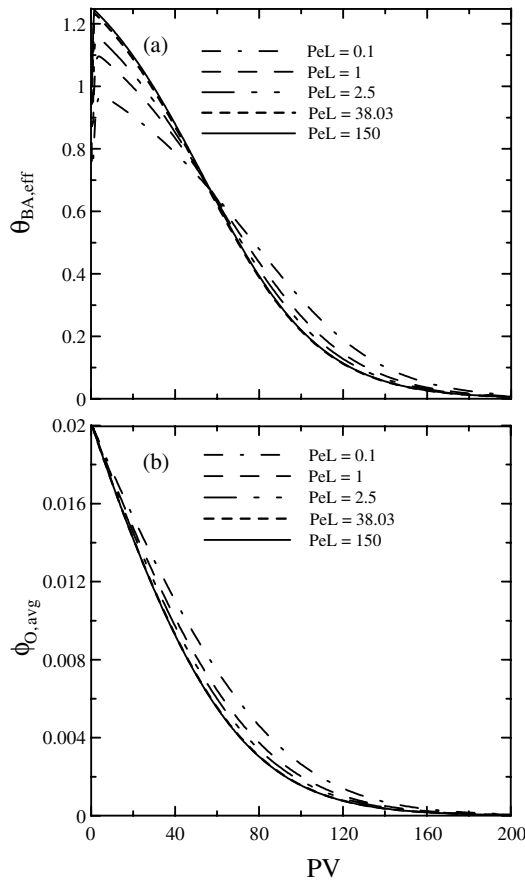
Fig. 5. Variations of $\theta_{BA,eff}$ and $\phi_{O,avg}$ with PV at various values of Pe_L for surfactant-enhanced solubilization in NAPL-contaminated columns. The other parameters are the same as those in Fig. 4 except the Pe_L value. Lines: prediction. — · — , — — , — ·· — , — — — — and ——— : Pe_L = 0.1, 1, 2.5, 38.03 and 150. (a) θ_{BA} and (b) $\phi_{O,avg}$.
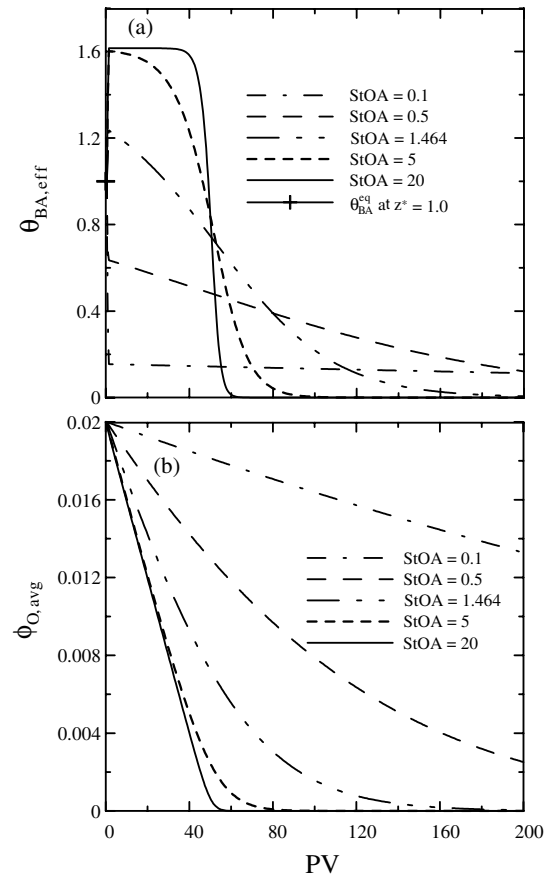
Fig. 6. Variations of $\theta_{BA,eff}$ and $\phi_{O,avg}$ with PV at various values of St_{OA} for surfactant-enhanced solubilization in NAPL-contaminated columns. The other parameters are the same as those in Fig. 4 except the St_{OA} value. Lines: prediction. — · — , — — , — ·· — , — — — — and ——— : St_{OA} = 0.1, 0.5, 1.464, 5, and 20. ╪╪ : θ_{BA}^{eq} at $z^* = 1.0$. (a) θ_{BA} and (b) $\phi_{O,avg}$.

same as those in Fig. 4. The different values of the Pe_L standing for the hydrodynamic conditions are presented by changing the α_L value. The $\theta_{BA,eff}$ would have the higher value in the initial stage and decrease faster with PV in the case of the greater Pe_L value (Fig. 5). It indicates that the hydrodynamic characteristic approaching to the plug flow is advantageous to the NAPL-aqueous mass transfer due to the higher concentration gradient of θ_{BA} along the column. Furthermore, the effect of the Pe_L value on the variations of the $\theta_{BA,eff}$ and $\phi_{O,avg}$ becomes slight when the Pe_L value is greater than 38.03.

Regarding the St_{OA} value adjusted by the k_1 value, it remarkably affects both $\theta_{BA,eff}$ and $\phi_{O,avg}$ (Fig. 6). The removal efficiencies of $\theta_{BA,eff}$ and $\phi_{O,avg}$ would significantly increase as the St_{OA} is enhanced. It reveals that the St_{OA} directly associated with the NAPL-aqueous mass transfer rate is an important factor for the remediation time. As illustrated in Fig. 6a, the $\theta_{BA,eff}$ value would be close to the θ_{BA}^{eq} when the St_{OA}

value equals to 20. That is considered in the solubility-limited regime while the NAPL-aqueous mass transfer rate is adequate for the θ_{BA} to reach the equilibrium value. Therefore, the greater St_{OA} value is desired for accelerating the decontamination efficiency.

In addition, the various MSR values can signify the surfactant-enhanced remediation system of different NAPL or surfactant. The variations of $\theta_{BA,eff}$ and $\phi_{O,avg}$ evidently depend on the MSR value as shown in Fig. 7. The $\theta_{BA,eff}$ value would dramatically raise with the increase of MSR because of the higher θ_{BA}^{eq} value as indicated in Eq. 1. When the MSR value is small like 0.01, the enhancement of the surfactant-enhanced solubilization for the remediation efficiency is insignificant. One may address that the presence of the surfactant in the remediation process accompanies the contribution of the MSR and the decrease of the k_1 value simultaneously. On the whole, the remediation rate of the contaminated soil would be enhanced by the addition of the surfactant.
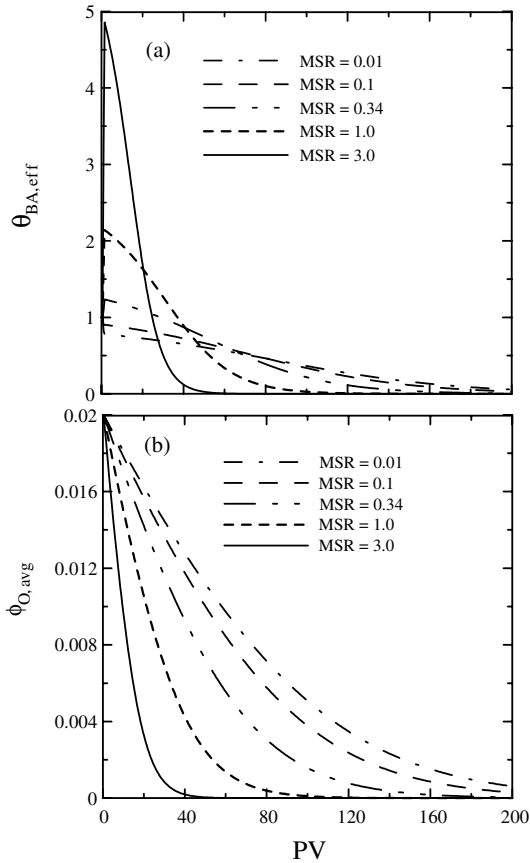
Fig. 7. Variations of $\theta_{BA,eff}$ and $\phi_{O,avg}$ with PV at various values of MSR for surfactant-enhanced solubilization in NAPL-contaminated columns. The other parameters are the same as those in Fig. 4 except the MSR value. Lines: prediction. ———, ———, ———, ————, and ————: MSR = 0.01, 0.1, 0.34, 1.0 and 3.0. (a) θ_{BA} and (b) $\phi_{O,avg}$.

CONCLUSIONS

1. The remediation of the TCE-contaminated soil is efficiently accelerated by the introduction of SDS-enhanced solubilization. In the experiments, the time for the complete remediation can be reduced more than 53% by flushing with the SDS-containing solution. The case of higher surfactant concentration or water flow rate would have the better remediation efficiency.

2. The injection of the surfactant-containing solution into the soil system needs about 1 to 3 PV for reaching the stabilization of the surfactant concentration. After the remediation process was started, the concentration and volumetric fraction profiles of TCE monotonically raising from the inlet to the outlet of the column decrease with the remediation time.

3. The present model considers the hydrodynamic

behavior, surfactant and organic solute concentrations, and TCE-aqueous mass transfer simultaneously. The dynamic variations of the effluent SDS and TCE concentrations can be well predicted during the remediation process. Moreover, the modified Sh for the TCE-aqueous mass transfer in the SDS-enhanced solubilization has the correlation of Sh = $30.3Re^{0.534}/(1 + 0.118(\theta_{SA}^{0})^{0.760})$.

4. The surfactant-enhanced solubilization system with the greater values of Pe_L and St_{OA}, and MSR is favorable for the remediation of the contaminated soil. Note that the time required for the complete elimination of pollutant can be reduced by increasing the values of Pe_L and St_{OA} and MSR

ACKNOWLEDGEMENTS

NOMENCLATURE

a_e	Specific NAPL-aqueous interfacial area based on the total volume, m^{-1}
$C_{BA}, C_{BA,eff}$	Concentrations of organic solute in bulk and effluent solutions, M or mg L^{-1}
C_{BO}	Concentration of organic solute in NAPL phase, M or mg L^{-1}
C_{cmc}	Critical micellar concentration of surfactant, M or mg L^{-1}
$C_e, \overline{C_e}$	Experimental data and the corresponding average value
C_p	Predicted values
$C_{SA}, C_{SA,eff}$	Surfactant concentration in bulk and effluent solutions, M or mg L^{-1}
C_{BA}^{eq}	Equilibrium concentration of organic solute in bulk solution, M or mg L^{-1}
C_{BW}^{sat}	Solubility of organic solute in water, M or mg L^{-1}
C_{BA}^{0}	Initial concentration of organic solute in bulk solution, M or mg L^{-1}
C_{SA}^{0}	Concentration of surfactant in influent solution, M or mg L^{-1}
d_p	Sand diameter, m
D_H	Hydrodynamic dispersion coefficient, $m^2 s^{-1}$, $\alpha_L v_A$
D_L	Diffusion coefficient of organic solute in aqueous solution, $m^2 s^{-1}$
k_f	NAPL-aqueous mass transfer coefficient of organic solute, m s^{-1}
k_L	Mass transfer coefficient of organic solute in liquid film, m s^{-1}
k_S	Mass transfer coefficient of organic solute

	in surfactant film, m s^{-1}
k_1	NAPL-aqueous mass transfer rate parameter, s^{-1}
L	Length of column, m
m	Constant of power
MSR	Molar solubilization ratio
NAPL	Non-aqueous phase liquid
Pe_L	Peclet number of aqueous phase, Lq/D_H
Pe_L^0	Pe_L at initial time
PV	Pore volumes, $t/(\phi_P t_L)$
q	Superficial velocity of aqueous phase, m s^{-1}
R^2	Determination coefficient, $1-[\sum(C_e-C_P)^2/\sum(C_e-\overline{C_e})^2]$
Re	Reynolds number defined in term of q, $d_p q/\nu_a$
S_A	Aqueous saturation, $\phi_A/(\phi_A + \phi_O)$
SDS	Sodium dodecyl sulfate
Sh	Modified Sherwood number, $k_1 d_p^2/D_L$ or $k_f a_e (S_A^3 - S_A^5)^{-1} d_p^2/D_L$
St_{OA}	NAPL-aqueous Stanton number of organic solute, $k_f a_e L/q$
St_{OA}^0	St_{OA} at initial time
t	Time, s
TCE	Trichloroethylene
TOCs	Total organic carbons
t_L	Hydraulic retention time, s, L/q
U_A	Dimensionless form of v_A, v_A/q
v_A	Actual velocity of aqueous phase, m s^{-1}, q/ϕ_A
z	Axial coordinate of column, m
z^*	Dimensionless form of z, z/L
α_L	Longitudinal dispersivity, m
$\theta_{BA}, \theta_{BA,eff}$	Dimensionless concentrations of organic solute in bulk and effluent solutions, C_{BA}/C_{BW}^{sat}, $C_{BA,eff}/C_{BW}^{sat}$
$\theta_{SA}, \theta_{SA,eff}$	Dimensionless concentrations of surfactant in bulk and effluent solutions, C_{SA}/C_{cmc}, $C_{SA,eff}/C_{cmc}$
θ_{BA}^{eq}	Dimensionless equilibrium concentration of organic solute in bulk solution, C_{BA}^{eq}/C_{BW}^{sat}
θ_{BA}^0	θ_{BA} at initial time, C_{BA}^0/C_{BW}^{sat}
θ_{SA}^0	θ_{SA} in influent solution, C_{SA}^0/C_{cmc}
ν_a	Kinematic viscosity of water, m^2 s^{-1}
τ	Dimensionless time, t/t_L
ϕ_A	Volume fraction of aqueous phase
ϕ_O	Volume fraction of NAPL
$\phi_{O,avg}$	Average value of ϕ_O along column
ϕ_P	Volume fraction of porosity
ϕ_O^0	ϕ_O at initial time

REFERENCES

1. Zimmerman, J.B., T.C.G. Kibbey, M.A. Cowell and K.F. Hayes, Paritioning of ethoxylated nonionic surfactants into nonaqueous-Phase organic liquids: influence on solubilization behavior. Environ. Sci. Technol., 33(1), 169-176 (1999).

2. Chu, M., P.K. Kitanidis and P.L. McCarty, Possible factors controlling the effectiveness of bioenhanced dissolution of non-aqueous phase tetrachloroethene. Adv. Water Resour., 27(6), 601-615 (2004).

3. Finkel, M., R. Liedl and G. Teutsch, Modelling surfactant-enhanced remediation of polycyclic aromatic hydrocarbons. Environ. Modell. Softw., 14(2-3), 203-211 (1999).

4. Sahloul, N.A., M.A. Ioannidis and I. Chatzis, Dissolution of residual non-aqueous phase liquids in porous media: Pore-scale mechanisms and mass transfer rates. Adv. Water Resour., 25(1), 33-49 (2002).

5. Ji, W. and M.L. Brusseau, A general mathematical model for chemical-enhanced flushing of soil contaminated by organic compounds. Water Resour. Res., 34(7), 1635-1648 (1998).

6. Lee, M., H. Kang and W. Do, Application of nonionic surfactant-enhanced in situ flushing to a diesel contaminated site. Water Res., 39(1), 139-146 (2005).

7. Vane, L.M., L. Hitchens, F.R. Alvarez and E.L. Giroux, Field demonstration of pervaporation for the separation of volatile organic compounds from a surfactant-based soil remediation fluid. J. Hazard. Mater., 81(1-2), 141-166 (2001).

8. Matheson, I.B.C. and A.D. King, Solubility of gases in micellar solutions. J. Colloid Interf. Sci., 66(3), 464-469(1978).

9. An, Y.J., E.R. Carraway and M.A. Sclautman, Solubilization of polycyclic aromatic hydrocarbons by perfluorinated surfactant micelles. Water Res., 36(1), 300-308 (2002).

10. Kim, E.S., D.H. Lee, B.W. Yum and H.W. Chang, The effect of ionic strength and hardness of water on the non-ionic surfactant-enhanced remediation of perchloroethylene contamination. J. Hazard. Mater., 119(1-3), 195-203 (2005).

11. Russell, H.H., J.E. Matthews and G.W. Sewell, TCE Removal from Contaminated Soil and Ground Water. United States Environmental Protection Agency, EPA/540/S-92/002, Washington, DC (1992).

12. United States Environmental Protection Agency, Trichloroethylene, Technology Transfer Network, Air Toxics Web Site. http://www.epa.gov/ttn/atw/hlthef/tri-ethy.html#ref (2007).

13. Loraine, G.A., Effects of alcohols, anionic and nonionic surfactants on the reduction of PCE and

TCE by zero valent iron, Water Res. 35(6), 1453-1460 (2001).

14. Zhang, C.L., G. Zheng and C.M. Nichols, Micellar partitioning and its effects on Henry's law constants of chlorinated solvents in anionic and nonionic surfactant solutions. Environ. Sci. Technol., 40(1), 208-214 (2006).

15. Abriola, L.M., T.J. Dekker and K.D. Pennell, Surfactant-enhanced solubilization of residual dodecane in soil columns. 2. Mathematic modeling. Environ. Sci. Technol., 27(12), 2341-2351 (1993).

16. Mason, A.R. and B.H. Kueper, Numerical simulation of surfactant-enhanced solubilization of pooled DNAPL. Environ. Sci. Technol., 30(11), 3205-3215 (1996).

17. Taylor, T.P., K.M. Rathfelder, K.D. Pennell and L.A. Abriola, Effects of ethanol addition on micellar solubilization and plume migration during surfactant enhanced recovery of tetrachloroethene. J. Contam. Hydrol., 69(1-2), 73-99 (2004).

18. Chen, Y.H., C.Y. Chang, Y.H. Yu, P.C. Chiang, C.Y. Chiu, Y. Ku and J.N. Chen, A dynamic model of ozone disinfection in a bubble column with oxygen mass transfer. J. Chin. Inst. Chem. Eng., 33(3), 253-265 (2002).

19. Sabatini, D.A., R.C. Knoxa and J.H. Harwell, Surfactant-Enhanced DNAPL Remediation: Surfactant Selection, Hydraulic Efficiency, and Economic Factors. United States Environmental Protection Agency, EPA/600/S-96/002, Washington, DC (1996).

20. Schwarzenbach, R.P., P.M. Gschwend and D.M. Imboden, Environmental Organic Chemistry. John Wiley & Sons, Inc., New York (1993).

21. Schaerlaekens, J., J. Vanderborght, R. Merckx and J. Feyen, Surfactant enhanced solubilization of residual trichloroethene: an experimental and numerical analysis. J. Contam. Hydrol., 46(1-2), 1-16 (2000).

22. Sanchez-Camazano, M., M.J. Sanchez-Martin and M.S. Rodriguez-Cruz, Sodium dodecyl sulphate-enhanced desorption of atrazine: effect of surfactant concentration and of organic matter content of soils. Chemosphere, 41(8), 1301-1305 (2000).

23. Casey, F.X.M., S.K. Ong and R. Horton, Degradation and transformation of trichloroethylene in miscible displacement experiments through zerovalent metals. Environ. Sci. Technol., 34(23), 5023-5029 (2000).

24. Ouyang, Y., J.S. Cho and R.S. Mansell, Simulated formation and flow of microemulsions during surfactant flushing of contaminated soil. Water Res., 36(1), 33-40 (2002).

25. Mayer, A.S., L. Zhong and G.A. Pope, Measurement of mass-transfer rates for surfactant-enhanced solubilization of nonaqueous phase liquids. Environ. Sci. Technol., 33(17), 2965-2972 (1999).

26. Zhong, L.R., A.S. Mayer and G.A. Pope, The effects of surfactant formulation on nonequilibrium NAPL solubilization. J. Contam. Hydrol., 60(1-2), 55-75 (2003).

27. Huang, H.L. and W.M.G. Lee, Enhanced naphthalene solubility in the presence of sodium dodecyl sulfate: effect of critical micelle concentration. Chemosphere, 44(5), 963-972 (2001).

28. Atta, K.R., D. Gavril, V. Loukopoulos and G. Karaiskakis, Study of the influence of surfactants on the transfer of gases into liquids by inverse gas chromatography, J. Chromatogr. A, 1023(2), 287-296 (2004).

29. Imhoff, P.T., P.R. Jaffe and G.F. Pinder, An experimental study of complete dissolution of a nonaqueous phase liquid in saturated porous media. Water Resour. Res., 30(2), 307-320 (1994).